Magnetic Penetration Depth Measurements of $Pr_{2-x}Ce_xCuO_{4-\delta}$ Films on Buffered Substrates: Evidence for a Nodeless Gap

Mun-Seog Kim, John A. Skinta, and Thomas R. Lemberger
Department of Physics, The Ohio State University, Columbus, Ohio 43210-1106, USA

A. Tsukada and M. Naito
NTT Basic Research Laboratories, 3-1 Morinosato Wakamiya, Atsugi-shi, Kanagawa 243, Japan
(Received 3 February 2003; published 19 August 2003)

We report measurements of the inverse squared magnetic penetration depth, $\lambda^{-2}(T)$, in $Pr_{2-x}Ce_xCuO_{4-\delta}$ ($0.115 \leq x \leq 0.152$) superconducting films grown on $SrTiO_3$ (001) substrates coated with a buffer layer of insulating Pr_2CuO_4. $\lambda^{-2}(0)$, T_c, and normal-state resistivities of these films indicate that they are clean and homogeneous. Over a wide range of Ce doping, $0.124 \leq x \leq 0.144$, $\lambda^{-2}(T)$ at low T is flat: it changes by less than 0.15% over a factor of 3 change in T, indicating a gap in the superconducting density of states. Fits to the first 5% decrease in $\lambda^{-2}(T)$ produce values of the minimum superconducting gap in the range of $0.29 \leq \Delta_{\min}/k_BT_c \leq 1.01$.

DOI: 10.1103/PhysRevLett.91.087001 PACS numbers: 74.20.Rp, 74.25.Ha, 74.72.Jt, 74.78.Bz

Determination of the pairing symmetry in novel superconductors is the essential first step in understanding the origin and nature of the superconducting state. Among the high-T_c cuprates, data on hole-doped compounds like $YBa_2Cu_3O_{7-\delta}$ and $La_{2-x}Sr_xCuO_4$ overwhelmingly indicate that pairing has d-wave symmetry [1,2]. This symmetry is expected theoretically, given that the undoped parent compounds are antiferromagnetic. However, in the closely related electron-doped cuprates, the pairing symmetry remains a puzzle [3–11]. Recently, novel concepts on pairing symmetry of n- and p-type cuprates have come forward: a possible transition in pairing symmetry [12,13] and/or a mixed symmetry order parameter [14–16].

Our previous work [12] involved $La_{2-x}Ce_xCuO_{4-\delta}$ (LCCO) and $Pr_{2-x}Ce_xCuO_{4-\delta}$ (PCCO) films grown directly on $SrTiO_3$ substrates. We found that at low Ce doping levels, $\lambda^{-2}(T)$ at low T was quadratic in T, but, at higher dopings, $\lambda^{-2}(T)$ showed activated behavior. These results suggested a d- to s-wave pairing transition near optimal doping, as was also suggested by tunneling experiments [13] on PCCO films. We have subsequently tried to improve film quality by eliminating the interface between the film and substrate, by growing PCCO films onto Pr_2CuO_4 (PCO)/$SrTiO_3$ instead of directly onto $SrTiO_3$. The insulating PCO layer should lessen lattice mismatch between PCCO film and $SrTiO_3$ substrate, so that these films should be more homogeneous through their thickness. In fact, their normal-state resistivities are somewhat lower than those of unbuffered PCCO films for the same doping, x. T_c's at optimal doping in the two film families are the same, $T_c \simeq 24$ K.

Films were prepared by molecular-beam epitaxy on 10 mm × 10 mm × 0.35 mm $SrTiO_3$ substrates as detailed elsewhere [17]. The same growth procedures and parameters were used for all films. For all films, PCCO and PCO layers are 750 and 250 Å thick, respectively. Ce concentrations, x, were measured to better than ± 0.005 by inductively coupled plasma spectroscopy. X-ray diffraction patterns for the films revealed that the c-axis lattice parameter monotonically decreases as in other electron-doped systems [18,19]. X-ray rocking curves showed full width at half maximum of (006) reflection for all films to be less than 0.4°, implying highly c-axis oriented films.

Four-circle x-ray diffraction measurements of a-axis lattice parameters for unbuffered and buffered films indicate that buffering reduces compressive strain due to the $SrTiO_3$ substrate ($a = 3.905$ Å). For example, for $x = 0.144$, the buffered film has a lattice parameter ($a = 3.9631$ Å) that is 0.2% larger than for the unbuffered film ($a = 3.9554$ Å). The c-axis lattice parameters of buffered and unbuffered films agree to 0.01%.

The penetration depth, $\lambda(T)$, was measured down to $T \simeq 0.5$ K using a mutual inductance apparatus, described in detail elsewhere [20,21], in a He^3 refrigerator. The system temperature was measured with a Cernox resistor (LakeShore Inc.) and its reliability, below 1 K, was confirmed by measuring the superconducting transition temperature of a Zn plate, $T_c = 0.875$ K.

Each film was centered between drive and pickup coils with diameters of ~1 mm. A small current at 50 kHz in the drive coil induced diamagnetic screening currents in the film. By symmetry, the electric field induced in the film (Faraday's law) lies in the plane of the film, i.e., parallel to the CuO_2 planes. Because films were much thinner than λ, the electric field in the films was essentially uniform through the film thickness. The time derivative of the net magnetic field from drive coil and induced current in the film was measured as a voltage across the pickup coil. The real and imaginary parts of the mutual inductance are proportional to the quadrature

and in-phase components of ac voltage, respectively. Because the coils were much smaller than the film, the applied field was concentrated near the center of the films, and demagnetizing effects at the film perimeter were not relevant. Nonlinear effects occur only very close to T_c where λ^{-2} is less than 1% of its value at $T = 0$. All data presented here represent linear response.

A numerical model of the drive and pickup coils enables us to convert the subtracted and normalized mutual inductance to *sheet* conductivity: $\sigma d = \sigma_1 d - i\sigma_2 d$, where d is film thickness. Finally, λ^{-2} is determined from $\sigma_2 d$ via $\sigma_2 = 1/\mu_0 \omega \lambda^2$, where μ_0 is the magnetic permeability of vacuum and ω is the angular frequency of the drive current. The absolute accuracy of λ^{-2} is limited by $\pm 10\%$ uncertainty in d. The T dependence of λ^{-2} is unaffected by this uncertainty. Systematic errors due to thermometry, the dielectric properties of helium-3 exchange gas, thermal expansion of coils, etc., are negligible. After averaging away Johnson noise in the electronics, residual noise in the measured value of $\lambda^{-2}(T)$ is about 0.1% of $\lambda^{-2}(0)$, coming largely from drift in the gain of our lock-in amplifiers.

Except for the flatness of $\lambda^{-2}(T)$ at low T, which is the focal point of this paper, buffered films are very much like unbuffered films reported earlier [12]. Figure 1 shows in-plane resistivity, $\rho_{ab}(T)$, for buffered PCCO films. ρ_{ab} in the normal state decreases smoothly and monotonically with Ce doping, x, even for small changes in x, implying that the main difference among films is Ce content. If there were random variations in degree of epitaxy, structural defects, etc., then resistivity would not be such a smooth function of x. These resistivities are slightly smaller than for PCCO films without buffer layers [11,12], and significantly lower than for NCCO and PCCO crystals [5,22]. The inset of Fig. 1 shows that resistive transitions are reasonably sharp, and that T_c is a weak function of Ce concentration, although resistivity is not. Table I summarizes properties of the films.

Fluctuations cause $\sigma_1(T)$ to peak at the superconducting transition. Hence, $\sigma_1(T)$ is a much more stringent test of film quality than resistivity. For example, if T_c varies through the film thickness, resistivity reveals only the highest T_c. Because our probing magnetic field passes through the film, $\sigma_1(T)$ has a peak at the T_c of every layer. Transitions associated with small bad spots in the film, as opposed to an entire film layer, are distinguished by their having essentially no effect on the superfluid response, σ_2. When a layer, not just a spot, goes superconducting there is a distinct change in the slope of $\lambda^{-2}(T)$.

$\sigma_1(T)$'s of buffered PCCO films (Fig. 2) show that several of them have a double transition, reflected as shoulder ($x = 0.115$, 0.124, and 0.137) or satellite ($x = 0.144$ and 0.152) structure of peaks. We define two transition temperatures, T_{c1} and T_{c2}, from peaks in $\sigma_1(T)$, where $T_{c1} > T_{c2}$. The resistive T_c is always at the onset of the T_{c1} peak. For the films most important to the conclusions of this Letter, $0.124 \leq x \leq 0.144$, the width of the T_{c1} peak, ΔT_{c1}, is ≤ 1 K, indicating excellent film homogeneity. The peak at T_{c2} most likely involves a bad spot in the film, since there is no corresponding feature in the slope of $\lambda^{-2}(T)$ (see Fig. 3). Accordingly, the lower transition is neglected in our analysis. Films with highest and lowest Ce concentrations ($x = 0.115$ and 0.152) have broader transitions ($\Delta T_c = 2.4$–3.9 K) than other films, perhaps because T_c is more sensitive to x.

Figure 3 shows $\lambda^{-2}(T)$ for all films. $\lambda^{-2}(0)$ vs x increases rapidly for $x \leq 0.133$, and it is constant or decreases slowly for $x > 0.133$. Values of $\lambda^{-2}(0)$ are slightly higher than for unbuffered films. The surprising upward curvature that develops in $\lambda^{-2}(T)$ near T_c at high Ce concentrations was also observed in unbuffered LCCO and PCCO films [11,12].

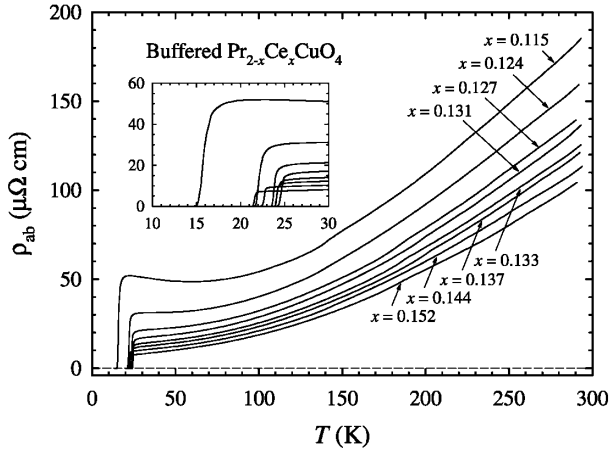

FIG. 1. *ab* plane resistivities, $\rho_{ab}(T)$, of buffered $Pr_{2-x}Ce_xCuO_{4-\delta}$ films. For resistivities at $T = 25$ K, see Table I. Inset: $\rho_{ab}(T)$ around T_c.

TABLE I. Properties of eight MBE-grown $Pr_{2-x}Ce_xCuO_{4-\delta}$ films on $Pr_2CuO_4/SrTiO_3$. T_c (or T_{c1}) and T_{c2} are locations of main and secondary peaks in $\sigma_1(T)$, respectively. ΔT_c is full width of the (main) peak in $\sigma_1(T)$. ρ_{ab} (25 K) is the *ab*-plane resistivity at $T = 25$ K. $\lambda^{-2}(0)$, $C_\infty/2$, and $D = \Delta_{\min}/k_B T_c$ are fit parameters, in Eq. (1).

x	T_c (T_{c1}) (K)	T_{c2} (K)	ΔT_c (K)	ρ_{ab}(25 K) ($\mu\Omega$ cm)	$\lambda^{-2}(0)$ (μm^{-2})	$C_\infty/2$	D
0.115	13.0	11.8	3.9	51.0	6.6	(0.21)	(0.29)
0.124	21.3	20.7	1.3	30.1	19.1	0.28	0.56
0.127	23.1		0.8	19.4	25.8	0.60	1.01
0.131	23.6		0.8	15.3	27.9	0.50	0.99
0.133	23.3		0.5	12.8	38.9	0.42	0.73
0.137	23.2	22.9	0.7	10.8	41.2	0.38	0.83
0.144	21.2	20.2	0.9	9.5	38.6	0.30	0.72
0.152	19.8	16.6	2.4	7.7	35.1	(0.17)	(0.37)

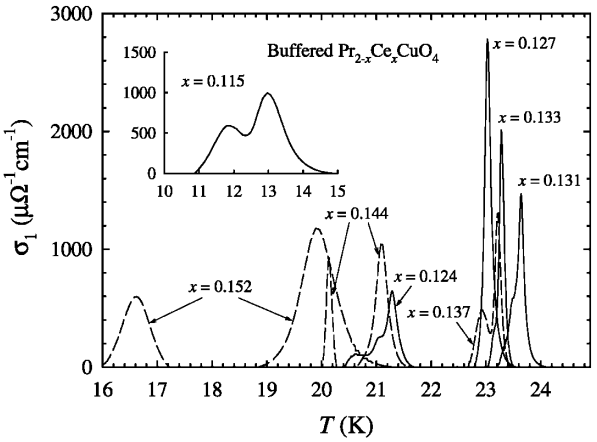

FIG. 2. $\sigma_1(T)$ at 50 kHz in buffered $Pr_{2-x}Ce_xCuO_{4-\delta}$ films. Inset: $\sigma_1(T)$ for the film with $x = 0.115$.

In our previous work [12] on unbuffered PCCO films, films with low Ce concentrations showed quadratic (T^2) behavior in $\lambda^{-2}(T)$ at low T. Films with high Ce concentrations showed gaplike behavior:

$$\lambda^{-2}(T) \simeq \lambda^{-2}(0)[1 - C_\infty \exp(-D/t)], \qquad (1)$$

where $\lambda^{-2}(0)$, C_∞, and D are adjustable parameters, and $t = T/T_c$. In the clean limit, D is approximately the minimum gap on the Fermi surface, normalized to k_BT_c, and C_∞ is roughly twice the average superconducting density of states (DOS) over energies within k_BT of the gap edge. For isotropic BCS superconductors, the best-fit value of $C_\infty/2$ is about 2.2, when the fit is limited to the first 5% drop in $\lambda^{-2}(T)$. The change in low-T behavior of $\lambda^{-2}(T)$ near optimal doping suggested a transition in pairing symmetry.

We now turn to the low-T behavior of $\lambda^{-2}(T)$ for buffered PCCO films, shown on a greatly expanded scale in Fig. 4. The most important thing to notice is that $\lambda^{-2}(T)$ is flat to better than 0.15% over a factor of 3 or more change in T. These data are incompatible with simple d-wave models with nodes in the gap. Thus, except for the most underdoped and overdoped films ($x = 0.115$ and 0.152), $\lambda^{-2}(T)$ shows gapped behavior. Recent angle-resolved photoemission spectroscopy measurements [4] indicate well-defined quasiparticle states on the Fermi surface where the $d_{x^2-y^2}$ node would be, so the gapped behavior that we observed cannot be ascribed to a Fermi surface or scattering effect.

To estimate the gap, we fit Eq. (1) to the first ~5% drop in $\lambda^{-2}(T)$ (thin solid lines in Fig. 4). It comes as no surprise that quadratic fits over the same temperature range are unacceptable (dashed lines). For films with $x = 0.115$ and 0.152, data are needed at temperatures below our current experimental limit of 0.5 K in order to distinguish between T^2 and $e^{-D/t}$. Values of the minimum gap, $\Delta_{\min} = Dk_BT_c$ and average DOS at the gap edge, $C_\infty/2$, extracted from the above exponential fits are presented in Table I. D values are significantly lower than the BCS weak-coupling-limit value, 1.76, for s-wave superconductors (2.14 for d-wave superconductors). D is largest, $D \sim 1$, for x near 0.13. We note that a similar value, $D \simeq 0.85$, was found for unbuffered PCCO films [11] with the same Ce concentration. Values of $C_\infty/2$ ($\ll 1$) are

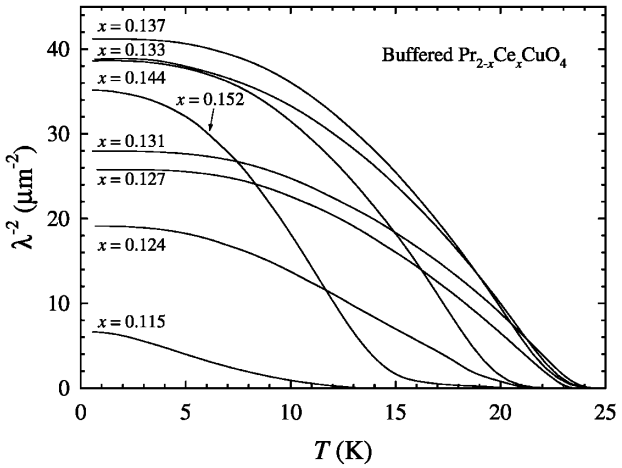

FIG. 3. $\lambda^{-2}(T)$ for buffered $Pr_{2-x}Ce_xCuO_{4-\delta}$ films. Film-to-film uncertainty in $\lambda^{-2}(0)$ is $\sim \pm 10\%$.

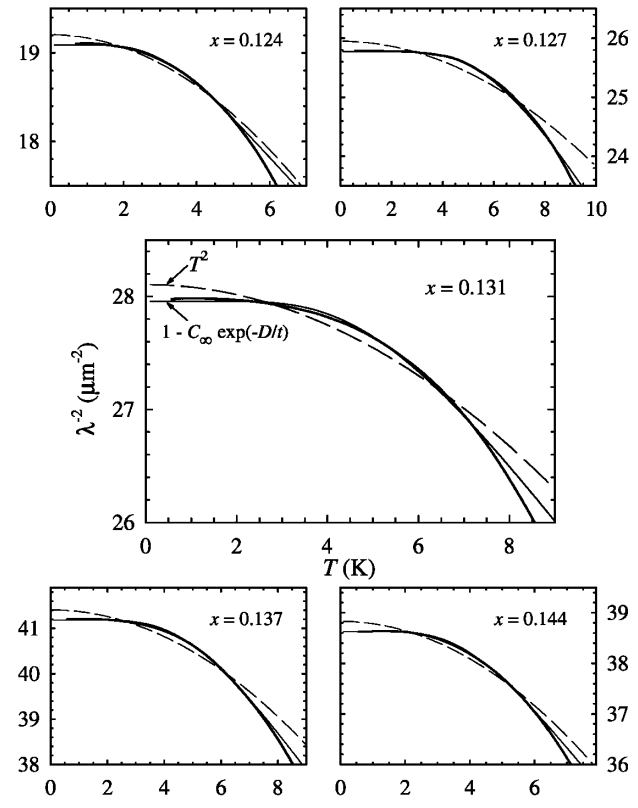

FIG. 4. Expanded view of $\lambda^{-2}(T)$ at low T for buffered $Pr_{2-x}Ce_xCuO_{4-\delta}$ films. Thin solid and dashed lines denote best fits of $\lambda^{-2}(0)[1 - C_\infty \exp(-D/t)]$ and $\lambda^{-2}(0)[1 - (T/T_0)^2]$ to the first 5% drop in $\lambda^{-2}(T)$, respectively.

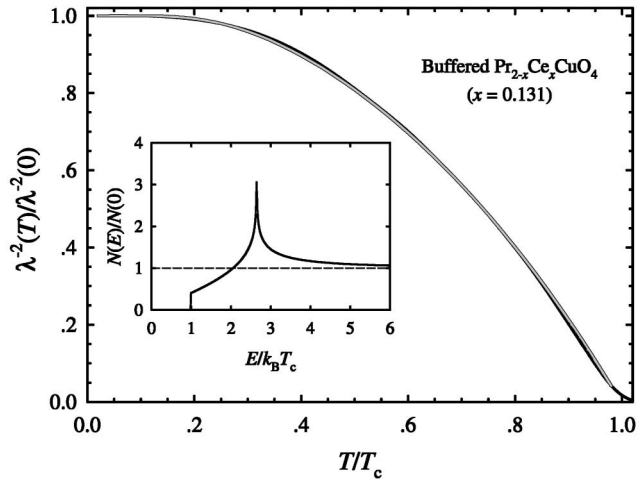

FIG. 5. $\lambda^{-2}(T)$ for $Pr_{1.869}Ce_{0.131}CuO_{4-\delta}$ film. Gray line shows an excellent fit obtained with density of states shown in the inset. Inset: Quasiparticle density of states in $s + id_{x^2-y^2}$ gap symmetry.

also much smaller than for weak-coupling isotropic s wave.

The gap and suppressed density of states at the gap edge imply that low-energy states have been pushed to higher energies to conserve states. We can ask: where is the peak in the DOS, i.e., how big is the maximum gap, $\Delta_{\max}$, on the Fermi surface? To answer this question, we fit the full T dependence of $\lambda^{-2}(T)$ by employing a model anisotropic gap function and the clean-limit result that $1 - \lambda^{-2}(T)/\lambda^{-2}(0)$ is an integral of quasiparticle DOS times the derivative of the Fermi function with respect to energy [23]. Figure 5 shows fits to the measured $\lambda^{-2}(T)$ for the film with $x = 0.131$ and $s + id_{x^2-y^2}$ gap: $|\Delta|^2 = [|\Delta_s|^2 + |\Delta_d|^2 \sin^2(2\phi)]$, where ϕ is the angle of the quasiparticle momentum. (The inset of Fig. 5 shows the quasiparticle DOS.) The best fit provides a reasonably good fit to the data, with a best-fit gap of $\Delta_{\max} \simeq 2.6 k_B T_c (\pm 15\%)$. In this fit, the minimum gap was fixed at the value found by fitting the low-T data alone, i.e., $\Delta_{\min}/k_B T_c = 0.99$. Then, as one can see in the inset of Fig. 5, the average DOS within $\sim k_B T$ of the minimum gap edge agrees well with $C_\infty/2 = 0.5$ from Table I.

We emphasize that we cannot say anything about the shape of the peak in the DOS, only its location. An equally acceptable fit, with a similar peak energy, is obtained even when the sharp narrow peak in the inset of Fig. 5 is replaced by a broad rectangular peak [24].

In summary, we measured the inverse squared magnetic penetration depth, $\lambda^{-2}(T)$, of several $Pr_{2-x}Ce_xCuO_{4-\delta}$ films on buffered $Pr_2CuO_4/SrTiO_3$ substrates down to $T/T_c < 0.03$. Overall, the resistivities and penetration depths were similar to films grown directly on $SrTiO_3$. However, for PCCO films on buffered substrates, $\lambda^{-2}(T)$ at low T exhibits gapped behavior over a wide range of Ce doping, including underdoping. This implies a superconducting gap without nodes on the Fermi surface. Values of the minimum superconducting gap for the films are in range of $0.3 \leq \Delta_{\min}/k_B T_c \leq 1.0$. We cannot distinguish among models with various gap symmetries, e.g., anisotropic s, $s + id$, or $d + id$. Our data are incompatible with the simple d-wave symmetry found in the closely related hole-doped cuprates.

The research at OSU was supported by NSF Grant No. DMR-0203739.

[1] D. J. VanHarlingen, Rev. Mod. Phys. **67**, 515 (1995).
[2] C. C. Tsuei and J. R. Kirtley, Rev. Mod. Phys. **72**, 969 (2000).
[3] C. C. Tsuei and J. R. Kirtley, Phys. Rev. Lett. **85**, 182 (2000).
[4] N. P. Armitage *et al.*, Phys. Rev. Lett. **86**, 1126 (2001).
[5] J. D. Kokales *et al.*, Phys. Rev. Lett. **85**, 3696 (2000).
[6] R. Prozorov, R.W. Giannetta, P. Fournier, and R. L. Greene, Phys. Rev. Lett. **85**, 3700 (2000).
[7] L. Alff *et al.*, Phys. Rev. B **58**, 11 197 (1998).
[8] S. Kashiwaya *et al.*, Phys. Rev. B **57**, 8680 (1998).
[9] C.-T. Chen *et al.*, Phys. Rev. Lett. **88**, 227002 (2002).
[10] L. Alff *et al.*, Phys. Rev. Lett. **83**, 2644 (1999).
[11] J. A. Skinta, T. R. Lemberger, T. Greibe, and M. Naito, Phys. Rev. Lett. **88**, 207003 (2002).
[12] J. A. Skinta *et al.*, Phys. Rev. Lett. **88**, 207005 (2002).
[13] A. Biswas *et al.*, Phys. Rev. Lett. **88**, 207004 (2002).
[14] K. A. Müller, Philos. Mag. Lett. **82**, 279 (2002).
[15] A. Kohen and G. Deutscher, cond-mat/0207382.
[16] D. Daghero, R. S. Gonnelli, G. A. Ummarino, and V. A. Stepanov, cond-mat/0207411.
[17] M. Naito, H. Sato, and H. Yamamoto, Physica (Amsterdam) **293C**, 36 (1997).
[18] M. Naito and M. Hepp, Jpn. J. Appl. Phys. Lett. **39**, 485 (2000).
[19] S. Karimoto, K. Ueda, M. Naito, and T. Imai, Appl. Phys. Lett. **79**, 2767 (2001).
[20] S. J. Turneaure, E. R. Ulm, and T. R. Lemberger, J. Appl. Phys. **79**, 4221 (1996).
[21] S. J. Turneaure, A. A. Pesetski, and T. R. Lemberger, J. Appl. Phys. **83**, 4334 (1998).
[22] J. D. Kokales *et al.*, Physica (Amsterdam) **341–348C**, 1655 (2001).
[23] M. Tinkham, *Introduction to Superconductivity* (McGraw-Hill, New York, 1996), 2nd ed.
[24] J. A. Skinta *et al.*, J. Low Temp. Phys. **131**, 359 (2003).